SCIENCE CHINA
Physics, Mechanics & Astronomy

• Article •

February 2013 Vol.56 No.2: 457–461
doi: 10.1007/s11433-012-4961-9

The influence of target material and thickness on proton energy and angular distribution†

SU LuNing[1], LIU BiCheng[1,2], LIN XiaoXuan[1], LIU Feng[1], DU Fei[1], LIU XiaoLong[1], ZHENG Yi[1], GE XuLei[1], LI YuTong[1*], SHENG ZhengMing[1,3], CHEN LiMing[1], WANG WeiMin[1], MA JingLong[1], LU Xin[1], WEI ZhiYi[1], CHEN JiaEr[2] & ZHANG Jie[1,3*]

[1] *Beijing National Laboratory for Condensed Matter Physics, Institute of Physics, Chinese Academy of Sciences, Beijing 100190, China;*
[2] *State Key Laboratory of Nuclear Physics and Technology, Institute of Heavy Ion Physics, Peking University, Beijing 100871, China;*
[3] *Key Laboratory for Laser Plasmas (Ministry of Education) and Department of Physics, Shanghai Jiao Tong University, Shanghai 200240, China*

Received October 26, 2012; accepted November 23, 2012; published online January 6, 2013

The paper has studied the influence of target material and thickness on energy and angular distributions of the protons generated by using an 800 nm, 60 fs, 0.24 J laser pulse to irradiate solid target foils. The results show that the initial density and thickness of the targets will affect the formation of the acceleration sheath fields in the target normal direction. For the same target thickness, using lower density target materials can obtain a higher proton maximum energy. However, lower density targets tend to be deformed due to the shock waves launched by the laser pulses, making the proton spatial distribution more divergent.

laser-driven, proton, acceleration

PACS number(s): 52.38.Kd, 52.50.Jm, 41.75.Jv

Citation: Su L N, Liu B C, Lin X X, et al. The influence of target material and thickness on proton energy and angular distribution. Sci China-Phys Mech Astron, 2013, 56: 457–461, doi: 10.1007/s11433-012-4961-9

1 Introduction

Energetic ion beams generated in the ultra-intense laser interactions with solid foils have wide applications in ion radiography [1], ion driven fast ignition [2], and medical therapy [3]. In recent years, laser driven ion accelerations have been widely studied under various experimental conditions, such as laser polarization [4,5], laser intensity [6], laser contrast ratio [7], plasma temperature [8], target thickness [9,10], plasma density [11,12], etc. A few acceleration mechanisms have been proposed, including shock acceleration [9,13,14], target normal sheath acceleration (TNSA) [15], Coulomb explosion acceleration [16,17], and radiation pressure acceleration [18]. Among them, the TNSA proposed by Wilks et al. [15] is one of the most important regimes of proton acceleration for the current laser conditions. In the mechanism, laser pulses interact with plasmas and generated hot electrons first. When the hot electrons are transported to the target rear surface, a sheath electric field is formed there, which then accelerates the ions in the target normal direction. Through the diagnosis of ion spectra in the target normal direction, many experiments have attempted to deduce the information of the target normal sheath field [19–21]. However, the source of hot electrons produced by the laser pulse has seldom been discussed.

*Corresponding author (LI YuTong, email: ytli@aphy.iphy.ac.cn; ZHANG Jie, email: jzhang@aphy.iphy.ac.cn)
†Contributed by CHEN JiaEr (CAS Academician) & ZHANG Jie (CAS Academician)

In this paper, we have performed an experiment on the femtosecond laser and solid foils interaction. According to the result of the experiment, in terms of electron transport and the formation of the target normal sheath field, using the TNSA model, we estimate the source of hot electrons and transverse scales of the target normal sheath field for different target materials and thicknesses. In addition, we have discussed the influence of ASE-generated shock waves on the divergent angle of protons.

2 Experimental setup

The experiments were conducted using the Xetreme Light (XL) II Ti: Sapphire laser system at the Institute of Physics in the Chinese Academy of Sciences. The XL-II laser system employs chirp pulse amplification (CPA) technology. The center wavelength is 800 nm, and the repetition frequency is 10 Hz. In most shots, laser pulses with energy of 200 mJ and duration of 60 fs were delivered onto the target foils. The contrast ratio measured by an ultrafast diode was about 10^{-6} nanoseconds before the main laser pulse. The experimental layout schematic is shown in Figure 1. A *p*-polarized laser main pulse was focused by an f/3.5 off-axis parabola (OAP) mirror onto the solid target obliquely at an incidence angle of 45°. The laser focal spot was oval, with a long and short axis 10 μm and 5 μm, respectively.

A 98 mm×49 mm×1 mm stack of CR-39, located 4 cm away from the target rear, was used to measure the angular distribution of the proton beams. Since CR-39 is insensitive to electrons and photons, we could obtain a proton angular distribution within 70 degrees behind the targets. A Thomson parabolic spectrograph 10 cm away from the target in the target normal direction was applied to measure the proton spectra. In the spectrograph, ions were deflected by a 2250 Gs magnetic field and a 1250 V electric field, and collected by a 49 mm×49 mm imaging plate. The collection angle of the spectrograph was 1.96×10^{-4} sr.

3 Results and discussion

We used 2 μm, 5 μm, and 10 μm thick Cu foil targets, and 0.65 μm, 2.5 μm, 4 μm, and 12.5 μm thick Al foil targets in our experiment. For the 0.65 μm thick Al target, the proton maximum energy is as high as 3.5 MeV. For the two target materials, proton energy always decreases with increasing target thickness. For example, in the case of a 12.5 μm thick Al target, the proton maximum energy is 1.25 MeV. Proton maximum energy versus target thickness is plotted in Figure 2. Meanwhile, we can see that the target material also affects the proton maximum energy. The proton maximum energies of a 2 μm Cu target and 5 μm Cu target are 1.5 MeV and 1.03 MeV, respectively. The proton maximum energies of a 2.5 μm Al target and 4 μm Al target, whose thicknesses are similar to the Cu targets above, are 2.9 MeV and 2.6 MeV.

The change of proton maximum energy could be explained by the TNSA mechanism. Hot electrons generated on the target front surface will propagate into the target. Hot electron temperature can be estimated by the ponderomotive potential,

$$T_{\rm hot} \approx m_{\rm e}c^2\left(\sqrt{1+a^2}-1\right), \tag{1}$$

where $a = I\lambda_{\mu\rm m}^2/1.37\times10^{18}$ is the normalized laser power density, I is the laser intensity, and $\lambda_{\mu\rm m}$ is the laser wavelength in the units of μm [22,23]. According to the laser energy loss, we can estimate the number of hot electrons, $N_{\rm e} = fE/T_{\rm hot}$, where E is laser energy and f is the laser energy absorption rate, typically in the range of 10%–40%. In

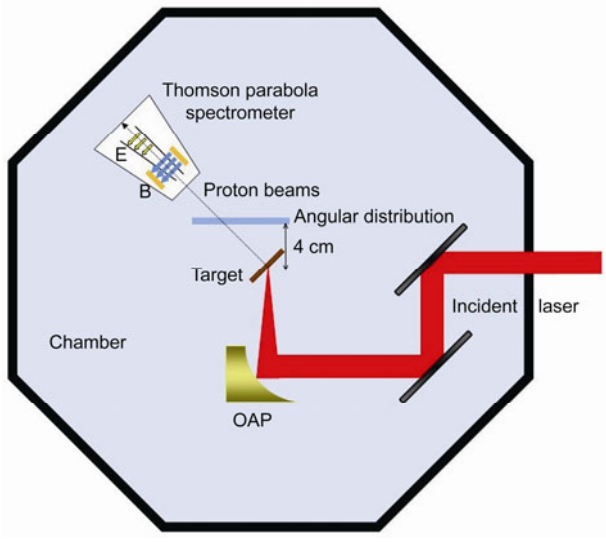

Figure 1 Experimental setup schematic.

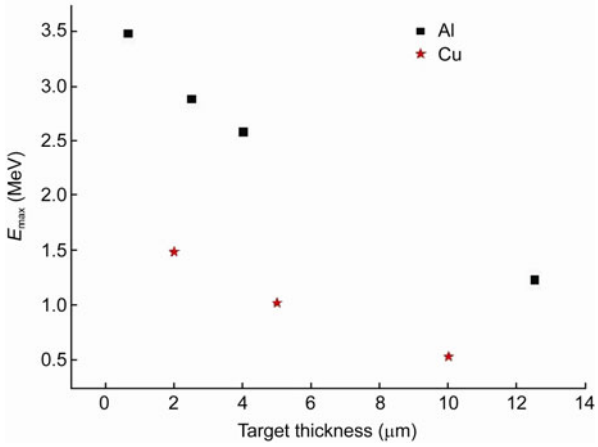

Figure 2 Proton maximum energy versus target thickness.

this estimation, we take f to be 35% [19]. When the hot electrons pass through the target, they can form the target normal sheath field at the target rear surface. Considering the influence of laser pulse duration, the electron density in the target normal sheath field can be $n_e = N_e / (DS)$, where $D = c\tau_{laser}$ is the electron sheath thickness [24], c is the light velocity, τ_{laser} is the laser pulse duration, $S = \pi(r + d\tan\theta)^2$ is the area of electron sheath, d is target thickness, r is laser focal spot radius, and θ is the electron sheath's half angle to the laser focal spot. Using the self-similar isothermal expansion fluid model, the proton maximum energy can be estimated by Mora's model [24, 25]

$$E_{max} = 2T_{hot}\left[\ln\left(t_p + \left(t_p^2 + 1\right)^{1/2}\right)\right]^2, \quad (2)$$

where normalized acceleration time t_p can be estimated using the ponderomotive potential $t_p = \omega_{pi} t_{acc} / (2e)^{1/2}$, $t_{acc} \approx 1.3\tau_{laser}$ is the interaction time [24], $\omega_{pi} = \left[\left(Z_i e^2 n_e\right) / \left(m_i \varepsilon_0\right)\right]^{1/2}$ is the ion plasma frequency, Z_i is the ion charge number, and m_i is the ion mass. According to the model above, we can use the proton maximum energy to calculate the value of θ. According to our experiment data, θ of different targets and of different target thicknesses are given in Table 1.

From Table 1, we can see two features. Firstly, for similar target thickness, the target normal sheath transverse area of Cu is larger than that of Al. Secondly, the sheath transverse area varies inversely with target thickness. When Al target thickness is small, θ is even less than zero degree, which means that the target normal sheath's area is less than the laser focal spot's area, and the hot electrons have been pinched by the target. This condition is consistent with the reference [19]. Honrubia et al. [26] found that the propagation of hot electrons in Al targets had three stages. (i) When hot electrons propagated in low density plasma, due to the interaction of the laser pulse with hot electrons, the transverse area of electron beams gradually grows larger. (ii) When hot electrons comes into the high density plasma, the laser will be reflected, electron beams will be pinched under the effect of self-generated magnetic field. (iii) However, when the pinch effect decreases, electron beams will diverge again. From this, we can infer that there is an optimal target thickness [7,27]. Under this optimal thickness, the transverse area of the target normal sheath is minimal; the electric field intensity of the target normal sheath is maximal, and then we can get the optimal proton maximum energy. According to our experiment data, an optimal target thickness obviously exists, and we can ensure that the optimal target thickness in our experiment is less than 2.5 μm.

Table 1 θ of different targets and different target thicknesses

	Thickness (μm)	Proton maximum energy (MeV)	θ (°)
Cu	10	0.54	20
Cu	5	1.03	15
Cu	2	1.5	4
Al	12.5	1.25	3
Al	4	2.6	–13.5
Al	2.5	2.9	–26
Al	0.65	3.5	–67

Figure 3 shows the proton angular distributions in our experiment, for different targets, 2 μm Cu, 5 μm Cu, 2.5 μm Al, and 4 μm Al, respectively. We can see that the size of beam spot decreases with increasing target thickness and target density. Meanwhile, the beam center is shifted to the laser propagation direction; the shifted distance is larger than that of a thick target. Besides the target normal sheath field area discussed above, the shock waves induced by the amplified spontaneous emission (ASE) of the laser pulses will also affect the divergence angle of the proton beams [28,29]. The ASE nanoseconds before the main pulse can form shock waves in the target front. When the shock waves propagate to the target rear, they will modify the target rear surface. Due to the TNSA mechanism, proton emission direction in the target rear has a close relationship with the proton wavefront profile [30], proton beams are always emitted along the local target normal direction [31]. As a result, the proton divergent angle depends on the degree of local convexity or fluctuation. The shock wave propagation velocity can be expressed as:

$$v = \frac{c_0}{2\alpha}\left(\sqrt{1 + \frac{4\alpha}{\rho_0 c_0^2} P} - 1\right), \quad (3)$$

where c_0 is the ion sound velocity, α is an empirical constant, $P = \eta I^{2/3}$ is shock wave pressure, η is nearly 1 as the laser wavelength is 800 nm, and ρ_0 is the initial target density. The duration time t_s of shock wave propagating from target front to target rear, depends on the plasma density and target thickness. As Cu density is larger than Al density, the t_s in the Cu target is longer than that in the Al target. Therefore, when the main pulse peak arrives at the target surface, the degree of convexity at the Cu target rear induced by the ASE is less than that of Al target, hence proton angular distribution of Cu targets is less divergent, and the shifting distance to laser propagation direction is also smaller comparing with the case of Al targets. On the other hand, t_s of the thicker target is longer than that of the thinner target, so proton angular distribution for the thicker target is also more concentrated. Consequently, in order to get proton beams with a low divergent angle, a high contrast laser is required to reduce the influence of shock waves.

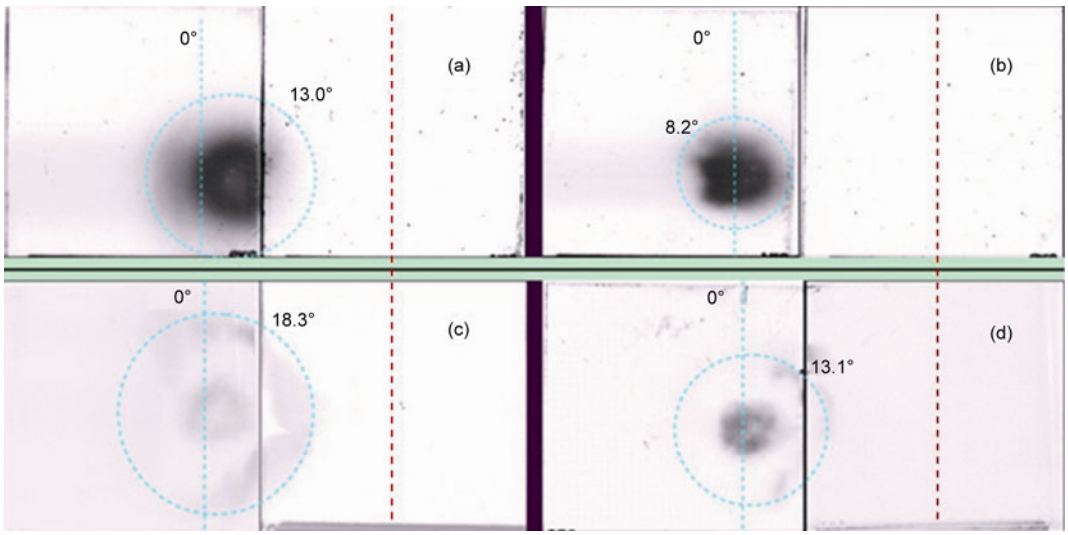

Figure 3 Proton angular distribution where the light blue dotted line is target normal direction and the red dotted line is laser propagation direction. The half angles of the proton beam sizes are labeled in each image. (a) 2 μm Cu; (b) 5 μm Cu; (c) 2.5 μm Al; (d) 4 μm Al.

4 Conclusion

We have studied the influence of target material and thickness on proton energy and angular distribution. The results show that proton beams with a maximum energy 3.5 MeV are generated in femtosecond laser and solid foils interactions. The maximum energy decreases with target thickness and with target initial density increasing. The divergent angle of fast electrons propagating inside the target and the induced transverse area of sheath field have been estimated. The proton divergent angle is believed to be mainly affected by the ASE-generated shock waves, which will decrease with target thickness and target initial density increasing.

This work was supported by the National Natural Science Foundation of China (Grant Nos. 10935002, 10925421, and 10974250), and the National Basic Research Program of China (973 Program, Grant No. 2007CB815102).

1 Borghesi M, Campbell D H, Schiavi A, et al. Electric field detection in laser-plasma interaction experiments via the proton imaging technique. Phys Plasmas, 2002, 9: 2214–2220
2 Kodama R, Norreys P A, Mima K, et al. Fast heating of ultra-high-density plasma as a step towards laser fusion ignition. Nature, 2001, 412: 798–802
3 Bulanov S S, Brantov A, Bychenkov V Y, et al. Accelerating protons to therapeutic energies with ultra-intense ultra-clean and ultra-short laser pulses. Med Phys, 2008, 35: 1770–1776
4 Zhang X M, Shen B F, Li X M, et al. Efficient GeV ion generation by ultraintense circularly polarized laser pulse. Phys Plasmas, 2007, 14: 123108
5 Yan X Q, Lin C, Sheng Z M, et al. Generating high-current monoenergetic proton beams by a circularly polarized laser pulse in the phase-stable acceleration regime. Phys Rev Lett, 2008, 100: 135003
6 Macchi A, Cattani F, Liseykina T V, et al. Laser acceleration of ion bunches at the front surface of overdense plasmas. Phys Rev Lett, 2005, 94: 165003
7 Kaluza M, Schreiber J, Santala M I K, et al. Influence of the laser prepulse on proton acceleration in thin-foil experiments. Phys Rev Lett, 2004, 93: 045003
8 Zhang X M, Shen B F, Yu M Y, et al. Effect of plasma temperature on electrostatic shock generation and ion acceleration by laser. Phys Plasmas, 2007, 14: 113108
9 Silva L O, Marti M, Davies J R, et al. Proton shock acceleration in laser-plasma interactions. Phys Rev Lett, 2004, 92: 015002
10 D'Humières E, Lefebvre E, Gremillet L, et al. Proton acceleration mechanisms in high-intensity laser interaction with thin foils. Phys Plasmas, 2005, 12: 062704
11 Wang X F, Nemoto K, Nayuki T, et al. Effect of plasma peak density on energetic proton emission in ultrashort high-intensity laser-foil interactions. Phys Plasmas, 2005, 12: 113101
12 Holkundkar A R, Gupta N K. Effect of initial plasma density on laser induced ion acceleration. Phys Plasmas, 2008, 15: 123104
13 Chen M, Sheng Z M, Dong Q L, et al. Ion acceleration by colliding electrostatic shock waves in laser-solid interaction. Phys Plasmas, 2007, 14: 113106
14 Chen M, Sheng Z M, Dong Q L, et al. Collisionless electrostatic shock generation and ion acceleration by ultraintense laser pulses in overdense plasmas. Phys Plasmas, 2007, 14: 053102
15 Wilks S C, Langdon A B, Cowan T E, et al. Energetic proton generation in ultra-intense laser-solid interactions. Phys Plasmas, 2001, 8: 542–549
16 Nakamura T, Fukuda Y, Yogo A, et al. High energy negative ion generation by Coulomb implosion mechanism. Phys Plasmas, 2009, 16: 113106
17 Murakami M, Mima K. Efficient generation of quasimonoenergetic ions by Coulomb explosions of optimized nanostructured clusters. Phys Plasmas, 2009, 16: 103108
18 Esirkepov T, Borghesi M, Bulanov S V, et al. Highly efficient relativistic-ion generation in the laser-piston regime. Phys Rev Lett, 2004, 92: 175003
19 Santos J J, Debayle A, Nicolaï Ph, et al. Fast-electron transport and induced heating in aluminum foils. Phys Plasmas, 2007, 14: 103107
20 Manclossi M, Santos J J , Batani D, et al. Study of ultraintense laser-produced fast-electron propagation and filamentation in insulator and metal foil targets by optical emission diagnostics. Phys Rev Lett, 2006, 96: 125002

21 Santos J J, Amiranoff F, Baton S D, et al. Fast electron transport in ultraintense laser pulse interaction with solid targets by rear-side self-radiation diagnostics. Phys Rev Lett, 2002, 89: 025001
22 Malka G, Miquel J L. Experimental confirmation of ponderomotive-force electrons produced by an ultrarelativistic laser pulse on a solid target. Phys Rev Lett, 1996, 77: 75–78
23 Wilks S C, Kruer W L, Tabak M, et al. Absorption of ultra-intense laser pulses. Phys Rev Lett, 1992, 69: 1383–1386
24 Fuchs J, Antici P, D'Humières E, et al. Laser-driven proton scaling laws and new paths towards energy increase. Nat Phys, 2006, 2: 48–54
25 Mora P. Plasma expansion into a vacuum. Phys Rev Lett, 2003, 90: 185002
26 Honrubia J, Kaluza M, Schreiber J, et al. Laser-driven fast-electron transport in preheated foil targets. Phys Plasmas, 2005, 12: 052708
27 Flacco A, Sylla F, Veltcheva M, et al. Dependence on pulse duration and foil thickness in high-contrast-laser proton acceleration. Phys Rev E, 2010, 81: 036405
28 Lindau F, Lundh O, Persson A, et al. Laser-accelerated protons with energy-dependent beam direction. Phys Rev Lett, 2005, 95: 175002
29 Lundh O, Lindau F, Persson A, et al. Influence of shock waves on laser-driven proton acceleration. Phys Rev E, 2007, 76: 026404
30 Brambrink E, Roth M, Blazevic A, et al. Modeling of the electrostatic sheath shape on the rear target surface in short-pulse laser-driven proton acceleration. Laser Part Beams, 2006, 24: 163–168
31 Xu M H, Li Y T, Liu F, et al. Enhancement of ion generation in low-contrast laser-foil interactions by defocusing. Acta Phys Sin, 2011, 60: 045204